

Novel B -decay signatures of light scalars at high energy facilities

Andrew Blance^{ab}, Mikael Chala^{ac}, Maria Ramos^d and Michael Spannowsky^a

^a*Institute of Particle Physics Phenomenology, Physics Department, Durham University, Durham DH1 3LE, UK*

^b*Institute for Data Science, Durham University, Durham DH1 3LE, UK*

^c*CAFPE and Departamento de Física Teórica y del Cosmos, Universidad de Granada, E18071 Granada, Spain*

^d*Laboratório de Instrumentação e Física Experimental de Partículas, Departamento de Física da Universidade do Minho, Campus de Gualtar, 4710-057 Braga, Portugal*

We study the phenomenology of light scalars of masses m_1 and m_2 coupling to heavy flavour-violating vector bosons of mass m_V . For $m_{1,2} \lesssim$ few GeV, this scenario triggers the rare B meson decays $B_s^0 \rightarrow 3\mu^+3\mu^-$, $B^0 \rightarrow 3\mu^+3\mu^-$, $B^+ \rightarrow K^+3\mu^+3\mu^-$ and $B_s^0 \rightarrow K^0*3\mu^+3\mu^-$; the last two being the most important ones for $m_1 \sim m_2$. None of these signals has been studied experimentally; therefore we propose analyses to test these channels at the LHCb. We demonstrate that the reach of this facility extends to branching ratios as small as 6.0×10^{-9} , 1.6×10^{-9} , 5.9×10^{-9} and 1.8×10^{-8} for the aforementioned channels, respectively. For $m_{1,2} \gg \mathcal{O}(1)$ GeV, we show that slightly modified versions of current multilepton and multitau searches at the LHC can probe wide regions of the parameter space of this scenario. Altogether, the potential of the searches we propose outperform other constraints such as those from meson mixing.

Contents

I. Introduction	1
II. Framework	2
III. Low mass regime at the LHCb	4
IV. High mass regime at the LHC	6
V. Conclusions	8
Acknowledgments	9
A. Concrete composite Higgs model	9
References	10

I. INTRODUCTION

Searches for new physics in final states often considered as “standard candles”, most notably in searches for supersymmetry (SUSY), have not provided any evidence of physics beyond the Standard Model (BSM) so far. This fact does not necessarily disproves low energy SUSY or other popular BSM extensions [1], such as composite Higgs models (CHM) [2, 3]. However, it supports the search for new physics in radically new and still unexplored channels.

In this paper we focus on light singlet scalars $a_{1,2}$ that can be produced in rare decays of B mesons mediated by heavy flavour-violating vector bosons V . This scenario is especially motivated, as it arises naturally in non-minimal CHMs [4–9]. (V and $a_{1,2}$ can be seen as the counterparts of the ρ and the pions in QCD.) Likewise,

such vector boson can explain the apparent anomalies observed in tests of lepton flavour universality [10–17]. Moreover, the bounds on such vector boson are weakened when it decays into lighter composite resonances [17], such as the aforementioned scalars. Finally, also supersymmetric models can trigger similar decays, mediated by scalar and pseudoscalar sgoldstino particles [18].

If, similarly to the Higgs boson, the scalars couple stronger to the muon than to the electron, processes such as $B_s^0 \rightarrow a_1 a_2$ can lead to four muon final states. To the best of our knowledge, the corresponding signal has been studied experimentally only at the LHCb [19]; the most stringent limit being $\mathcal{B}(B_s^0 \rightarrow 2\mu^+2\mu^-) < 2.5 \times 10^{-9}$.

However, there are different reasons to consider alternative B meson decay modes. To start with, the partial width for $a_2 \rightarrow a_1 a_1$ can very easily dominate over the corresponding leptonic width. In this case, six muon final states rather than four muon ones are to be studied. And secondly, the scalars couple to the mediator as a vector current $\sim a_1 \partial a_2$. When the latter is conserved, namely for $m_1 \sim m_2$ (and in particular in the massless limit), the B meson decay into such scalars vanishes. In other words, $\Gamma(B_s^0 \rightarrow a_1 a_2) \sim (m_1^2 - m_2^2)/m_B$. In this regime, one should rather explore three body decays of B with emitted mesons. In this work we focus mostly on $B^+ \rightarrow K^+3\mu^+3\mu^-$. (The inclusion of conjugate modes of charged decays is implied throughout the paper.)

We also extend previous works on this topic [18, 20, 21] by studying the regime of large scalar masses. In such regime, $a_{1,2}$ can no longer show up in rare decays of B mesons. However, they can appear in decays of the vector mediator if it is at the TeV scale and therefore be produced in pp collisions at the LHC.

This article is organised as follows. In section II, we provide the Lagrangian relevant for our study and define

the region of the parameter space of phenomenological interest. In section III we focus on the regime $m_{1,2} \lesssim$ few GeV and provide analyses for the LHCb and estimate the reach for different B decays. We do not circumscribe to any particular value of $m_{1,2}$, but rather scan over different values of these. In section IV we focus instead on the regime $m_{1,2} >$ few GeV and study the corresponding LHC signatures.

Unless otherwise stated, all limits given in this article stand for 95% CL.

We conclude in section V, while we dedicate Appendix A to building a complete model that predicts definite values of several of the parameters that we scan over.

II. FRAMEWORK

Let us consider the Lagrangian of the SM extended with a heavy vector V , and two light scalars a_1, a_2 . The relevant Lagrangian before electroweak symmetry breaking (EWSB) (in the basis in which up quark and lepton Yukawas are diagonal) reads

$$L = \frac{1}{2}m_V^2 V_\mu V^\mu + \frac{1}{2}m_1^2 a_1^2 + \frac{1}{2}m_2^2 a_2^2 + m_{12}a_2 a_1^2 + \dots + V^\mu \left[g_{12}a_1 \overleftrightarrow{\partial}_\mu a_2 + g_{qq}(\overline{qL}\gamma_\mu q_L + \text{h.c.}) \right], \quad (1)$$

with $m_V \gg m_{1,2}$. The ellipsis stand for terms not relevant for this study. Without loss of generality, we assume $m_2 > m_1$. The scalars $a_{1,2}$ can be more naturally thought of as the real and imaginary components of a complex field Φ ; the Lagrangian being invariant under $\Phi \rightarrow \exp(i\theta)\Phi$ up to $\mathcal{O}(1 - m_2/m_1, m_{12})$. In the Appendix A we match a concrete CHM to the Lagrangian above.

Assuming that V interacts mostly with the third generation quarks, after EWSB it couples to $\overline{b}_L b_L$ and $\overline{t}_L t_L$ as well as $\overline{b}_L s_L + \text{h.c.}$ with strengths $\sim g_{qq}$ and

$$g_{sb} \equiv g_{qq} V_{ts}^{CKM} V_{tb}^{CKM} \sim 0.04 g_{qq}, \quad (2)$$

respectively.

We distinguish two different regimes depending on the masses of the scalars: $1 \text{ GeV} \lesssim m_{1,2} \lesssim 4 \text{ GeV}$ (*low mass regime*) and $m_{1,2} > 4 \text{ GeV}$ (*high-mass regime*). Likewise, we consider two possible scenarios for the couplings of $a_{1,2}$ to the fermions. First, we assume that $a_{1,2}$ are muonphilic. As a second possibility, we assume that they couple only to the SM leptons and with Higgs-like strength, namely $\sim g_{1,2}y_\ell a_{1,2} \ell^+ \ell^-$, with y_ℓ the SM Yukawa couplings and $g_{1,2}$ free dimensionless parameters and lepton independent.

In the *low-mass regime*, a_1 decays mostly into muons irrespectively of whether it is muonphilic or just leptonphilic. In the *high-mass regime*, it decays mostly into taus unless it is muonphilic.

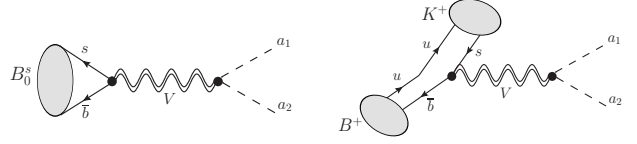


FIG. 1: *Tree level Feynman diagram for the decays $B_s^0 \rightarrow a_1 a_2$ (left) and $B^+ \rightarrow K^+ a_1 a_2$ (right).*

Regarding the decay of a_2 , if $m_2 > 2m_1$, then a_2 can either decay into $a_1 a_1$ or into lepton pairs, depending on m_{12}/g_2 :

$$\Gamma(a_2 \rightarrow \ell^+ \ell^-) = \frac{g_2^2 y_\ell^2}{8\pi} \left(1 - \frac{4m_\ell^2}{m_2^2}\right)^{3/2} m_2, \quad (3)$$

$$\Gamma(a_2 \rightarrow a_1 a_1) = \frac{m_{12}^2}{8\pi m_2} \left(1 - \frac{4m_1^2}{m_2^2}\right)^{1/2}. \quad (4)$$

In what follows, we assume that $m_{12}/m_2 \gg g_2 y_\ell$ in this regime, so that $\mathcal{B}(a_2 \rightarrow a_1 a_1) \gg \mathcal{B}(a_2 \rightarrow \ell^+ \ell^-)$. Note that this inequality holds almost trivially, since one expects $m_{12} \sim m_2$ whereas the Yukawas are tiny.

If instead $m_2 < 2m_1$, a_2 can either decay into pairs of leptons as before, or into $a_1 \ell^+ \ell^-$ with width

$$\Gamma(a_2 \rightarrow a_1 \ell^+ \ell^-) \sim \frac{(g_1 y_\ell)^2}{64\pi^3 m_2^3} m_{12}^2 m_1^2 \left(1 + \frac{m_2}{m_1}\right) \left(\frac{m_2}{m_1} - 1\right)^5. \quad (5)$$

This decay mode dominates if $g_1 \gtrsim 100g_2$. We assume this hierarchy hereafter. Thus, for example for $g_1 = 3$ and $g_2 = 0.01$, a_2 decays always into four leptons mediated by a_1 , which can be either on-shell or off-shell. Also, they both have widths smaller than 10 MeV and lifetime shorter than 10 fs. As a consequence, both $a_{1,2}$ would seem to have vanishing experimentally measurable widths and flight distances. Furthermore, note that the Yukawa suppression helps also avoiding bounds from BaBar and even the future Belle-II [22].

At low energies, the vector boson V triggers B meson decays into the light scalars; see Fig. 1. Depending on the relative size between m_B and $m_{1,2}$ we distinguish two cases:

- If $m_B > m_1 + m_2$, we have $B_s^0 \rightarrow a_1 a_2$.
- If $m_B < m_1 + m_2$ and $m_B > 3m_1$, we have instead $B_s^0 \rightarrow a_1 a_1 a_1$. (Other three body decays, e.g. $B_s^0 \rightarrow a_1 \mu^+ \mu^-$ are subdominant due to the Yukawa suppression.)

If $m_B > m_1 + m_2 + m_K$, we also have $B^+ \rightarrow K^+ a_1 a_2$. We do not consider any other cases in this paper; see Fig. 2.

The decay width for $B_s^0 \rightarrow a_1 a_2$ reads:

$$\Gamma = \frac{f_B^2}{16\pi m_V^4} (g_{sb} g_{12})^2 \frac{(m_1^2 - m_2^2)^2}{m_B} \mathcal{K}\left(\frac{m_1}{m_B}, \frac{m_2}{m_B}\right) \quad (6)$$

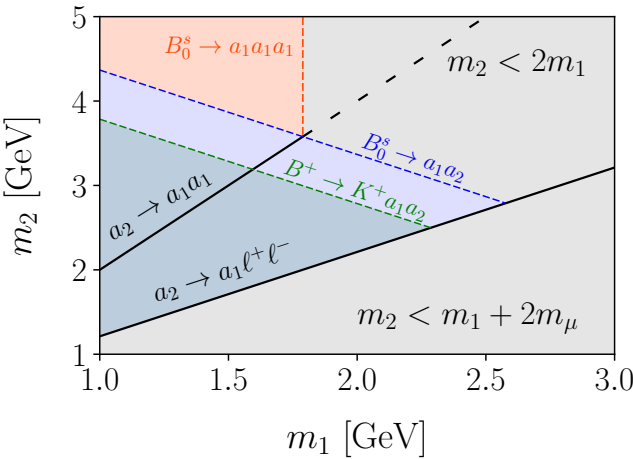


FIG. 2: Dominant decays taking place in the different regions of the plane (m_1, m_2) . The gray areas are not considered in this analysis.

with

$$\mathcal{K}(x, y) = \left[x^4 + (1 - y^2)^2 - 2x^2(1 + y^2) \right]^{1/2} \quad (7)$$

and $f_B \sim 0.23$ GeV [23].

The amplitude for $B_s^0 \rightarrow a_1 a_1 a_1$ reads:

$$\mathcal{M} = 2g_{sb}g_{12} \frac{f_B m_{12}}{m_V^2} \left[\frac{q_{12}^2 - m_1^2}{q_{12}^2 - m_2^2} + \frac{q_{23}^2 - m_1^2}{q_{23}^2 - m_2^2} + \frac{q_{13}^2 - m_1^2}{q_{13}^2 - m_2^2} \right], \quad (8)$$

where we have defined the transferred momenta $q_{12}^2 = (p_1 + p_2)^2$, $q_{23}^2 = (p_2 + p_3)^2$ and $q_{13}^2 = (p_1 + p_3)^2 = 3m_1^2 + m_B^2 - q_{12}^2 - q_{23}^2$. After integrating over q_{23}^2 , we obtain:

$$\frac{d\Gamma}{dq_{12}^2} = \frac{(g_{sb}g_{12})^2 m_2^2}{384\pi^3 m_B^3} \left(\frac{f_B m_{12}}{m_V^2} \right)^2 F \left[\frac{m_1}{m_2}, \frac{m_B}{m_2}, \frac{q_{12}}{m_2}, \frac{q_{23}}{m_2} \right]_{(q_{23}^2)_{\min}}^{(q_{23}^2)_{\max}} \quad (9)$$

with

$$F(x, y, w, v) = (1 - x^2)^2 \left[\frac{1}{1 - v^2} + \frac{1}{3x^2 + y^2 - w^2 - v^2 - 1} \right] + \frac{v^2 (2 + x^2 - 3w^2)^2}{(w^2 - 1)^2} + 2(x^2 - 1) \times \times \left\{ \frac{3x^4 + x^2(3 + y^2 - 9w^2) + y^2(2 - 3w^2) + 3(w^4 + w^2 - 1)}{(w^2 - 1)(3x^2 + y^2 - w^2 - 2)} [\log(v^2 - 1) - \log(1 + w^2 + v^2 - 3x^2 - y^2)] \right\} \quad (10)$$

which should be evaluated at

$$(q_{23}^2)^{\max} = (E_2^* + E_3^*)^2 - \left(\sqrt{E_2^{*2} - m_1^2} - \sqrt{E_3^{*2} - m_1^2} \right)^2$$

$$(q_{23}^2)^{\min} = (E_2^* + E_3^*)^2 - \left(\sqrt{E_2^{*2} - m_1^2} + \sqrt{E_3^{*2} - m_1^2} \right)^2, \quad (11)$$

where $E_2^* \equiv q_{12}/2$ and $E_3^* \equiv (m_B^2 - q_{12}^2 - m_1^2)/(2q_{12})$. The final width is obtained integrating over q_{12}^2 between $4m_1^2$ and $(m_B - m_1)^2$.

In the limit $m_1, m_2 \rightarrow 0$, the integrated width simplifies to:

$$\Gamma \sim \frac{3(g_{sb}g_{12})^2}{256\pi^3} \frac{f_B^2 m_{12}^2}{m_V^4 m_B^4} m_B. \quad (12)$$

Finally, the amplitude for $B^+ \rightarrow K^+ a_1 a_2$ is given by:

$$\mathcal{M} = -\frac{g_{sb}g_{12}}{m_V^2} \langle K(p_3) | \bar{s} \gamma_\mu b | B(p) \rangle (p_2 - p_1)^\mu, \quad (13)$$

with

$$\langle K(p_3) | \bar{s} \gamma_\mu b | B(p) \rangle = f_+(q^2) \left[(p + p_3)_\mu - \frac{m_B^2 - m_K^2}{q^2} q_\mu \right] + f_0(q^2) \frac{m_B^2 - m_K^2}{q^2} q_\mu \quad (14)$$

and again $q^2 = (p - p_3)^2$ is the transferred momentum, ranging from $(m_1 + m_2)^2 < q^2 < (m_B - m_K)^2$. The contraction of this matrix element with $(p_2 - p_1)$ in Eq. 13 simplifies to

$$\mathcal{M} = -\frac{g_{sb}g_{12}}{m_V^2} \left\{ \frac{(m_B^2 - m_K^2)(m_2^2 - m_1^2)}{q^2} [f_0(q^2) - f_+(q^2)] + \left[2(p_2 + p_3)^2 + q^2 - m_1^2 - m_2^2 - m_B^2 - m_K^2 \right] f_+(q^2) \right\}. \quad (15)$$

For convenience, we trade these variables for $M_{12}^2 \equiv m_2^2 - m_1^2$ and $M_{BK}^2 \equiv m_B^2 - m_K^2$, getting

$$\frac{d\Gamma}{dq^2} = \frac{(g_{sb}g_{12})^2}{768\pi^3 m_V^4 m_B^3} F(q^2), \quad (16)$$

with

$$F(q^2) = \frac{1}{q^2} \left[\frac{(M_{BK}^2 + q^2)^2}{q^4} - 4 \frac{m_B^2}{q^2} \right]^{1/2} \left[\frac{(M_{12}^2 + q^2)^2}{q^4} - 4 \frac{m_2^2}{q^2} \right]^{1/2} \times \left\{ 3M_{BK}^4 M_{12}^4 |f_0(q^2)|^2 + [q^4 + 2q^2 (M_{BK}^2 - 2m_B^2) + M_{BK}^4] [q^4 + 2q^2 (M_{12}^2 - 2m_2^2) + M_{12}^4] |f_+(q^2)|^2 \right\}. \quad (17)$$

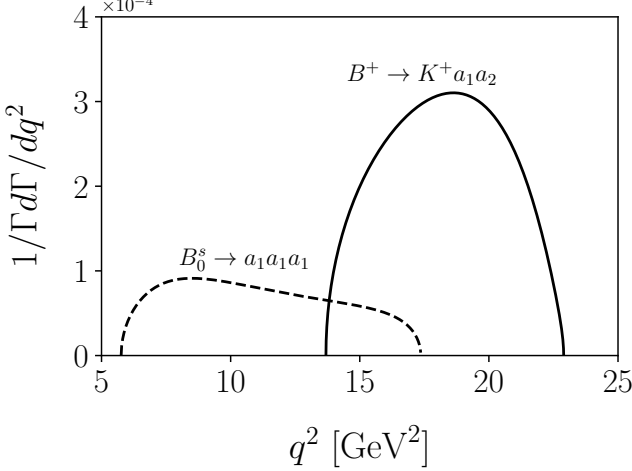


FIG. 3: Differential branching ratios as a function of $q^2 = (p_1 + p_2)^2$. We have fixed $m_1 = 1.2$ GeV, $g_{sb} = g_{12} = 1$, $m_V = 1$ TeV and $m_{12} = 5$ GeV. Due to the different kinematic regions where these decays take place, we have set $m_2 = 2.5$ GeV and $m_2 = 5$ GeV for the $B^+ \rightarrow K^+ a_1 a_2$ and $B_0^+ \rightarrow a_1 a_1 a_1$, respectively.

Following Ref. [24], we parameterize the form factor as

$$f_+(q^2) = \frac{r_1}{(1 - q^2/m^2)} + \frac{r_2}{(1 - q^2/m^2)^2}, \quad (18)$$

with $r_1 = 0.162$, $r_2 = 0.173$ and $m^2 = 5.41^2$ GeV². Similarly,

$$f_0(q^2) = \frac{r_2}{(1 - q^2/m_{\text{fit}}^2)} \quad (19)$$

with $r_2 = 0.330$ and $m_{\text{fit}}^2 = 37.46$ GeV². Finally, in the approximation $m_1, m_2, m_K \rightarrow 0$ and $f_0, f_+(q^2) \rightarrow 1$, we obtain:

$$\Gamma \sim \frac{(g_{sb} g_{12})^2}{3072 \pi^3 m_V^4} m_B^5. \quad (20)$$

In Fig. 3, we show the magnitude of three body decays under consideration and their dependence with $(p_1 + p_2)^2$.

In Fig. 4, we show the ratio of $\Gamma(B_s^0 \rightarrow a_1 a_2)$ to $\Gamma(B^+ \rightarrow K^+ a_1 a_2)$. It is very worth noting that it vanishes in the limit $m_1 \rightarrow m_2$; see also Eq. 6. In this regime, searches for B_s^0 decaying only to muons are irrelevant; extra mesons have to be tagged instead. There are however

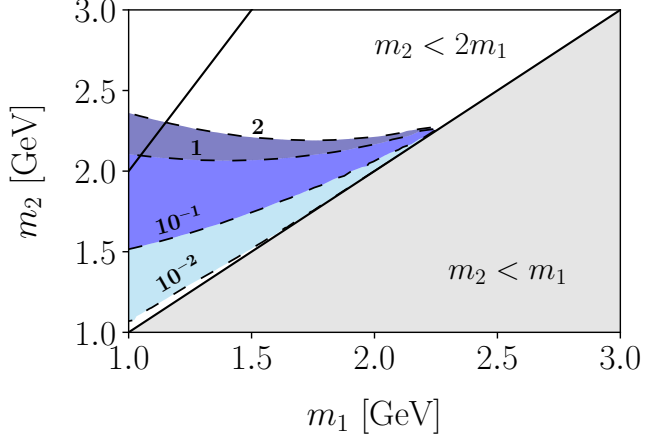


FIG. 4: Value of $\Gamma(B_s^0 \rightarrow a_1 a_2) / \Gamma(B^+ \rightarrow K^+ a_1 a_2)$ in the plane (m_1, m_2) . This ratio vanishes along the line $m_1 = m_2$.

no analyses (not even prospects) in this respect, and this is a gap that we try to overcome in this work.

At high energies, V can be produced on-shell in pp collisions initiated by bottom quarks, and subsequently decay into third generation quarks and into $a_1 a_2$ with respective widths:

$$\begin{aligned} \Gamma(V \rightarrow q\bar{q}) &= \frac{g_{qq}^2}{8\pi} \left(1 - \frac{m_q^2}{m_V^2} \right) \left(1 - \frac{4m_q^2}{m_V^2} \right)^{1/2} m_V, \\ \Gamma(V \rightarrow a_1 a_2) &= \frac{g_{12}^2}{48\pi} \left[1 - 2 \frac{m_1^2 + m_2^2}{m_V^2} + \frac{(m_2^2 - m_1^2)^2}{m_V^4} \right]^{3/2} m_V, \end{aligned} \quad (21)$$

with $q = t, b$. Note that the scalar decay mode dominates already for $g_{12} \gtrsim 3g_{qq}$.

III. LOW MASS REGIME AT THE LHCb

In the low mass regime, the smoking gun signature of the Lagrangian in Eq. 1 is rare decays of B mesons into final states containing six muons (and possibly other lighter mesons). Let us focus first on the channel $B_s^0 \rightarrow$

	$m_X \geq m_1 + m_2$	$m_X < m_1 + m_2$	
	$m_2 \geq 2m_1$	$m_2 < 2m_1$	$m_X \geq 3m_1$
$B_s^0 \rightarrow 3\mu^+3\mu^-$	[0.02,0.03]	[0.01,0.02]	[0.02,0.03]
limit ($\times 10^{-9}$)	[6.7, 11.6]	[7.9, 18.2]	[6.0, 11.9]
$B^+ \rightarrow K^+3\mu^+3\mu^-$	[0.007,0.009]	[0.003,0.009]	four-body
limit ($\times 10^{-9}$)	[5.9, 8.0]	[6.0, 16.6]	four-body

TABLE I: *Maximum and minimum efficiencies for selecting signal events in the channels $B_s^0 \rightarrow 3\mu^+3\mu^-$ ($m_X = m_{B_s^0}$) and $B^+ \rightarrow K^+3\mu^+3\mu^-$ ($m_X = m_{B^+} - m_{K^+}$) in each kinematic region. The upper limits ($\times 10^{-9}$) on the corresponding branching ratios for 3 fb^{-1} of data are also shown. We vary $m_{1,2}$ in the coloured region of Fig. 2, with $m_2 < 10 \text{ GeV}$ and $m_1 \geq 1.1 \text{ GeV}$. (For smaller values of m_1 the efficiency is negligible.)*

$3\mu^+3\mu^-$. As we have already commented, there are no searches for this decay mode, and so neither constraints nor any direct way to estimate the potential of the LHCb to test this process. We therefore suggest the first analysis in this respect.

We first require events with at least one muon with $p_T > 1.7 \text{ GeV}$; this cut ensures that the events pass the same hardware trigger used at $\sqrt{s} = 8 \text{ TeV}$ [19]. We subsequently require exactly six muons, with vanishing total charge. We also require all muon tracks to have $p_T > 0.5 \text{ GeV}$ and $2.5 < \eta < 5.0$. Finally, we require all muons tracks to have total momentum larger than 2.5 GeV to simulate the threshold for muon identification based on the penetration power through absorption plates in the detector.

Due to the six muons in the final state, the SM backgrounds are negligible to very good approximation. They arise mostly from resonant production of J/Ψ and φ with subsequent decays into muons; we completely remove them by enforcing that no zero charge muon pair has an invariant mass in the range $[0.95, 1.09] \cup [3.0, 3.2] \text{ GeV}$. (We lose sensitivity to signal events with m_1 in that region, though.) Even searches for four muons are background free [19, 21], so it is guaranteed that any observed event in the six lepton final state is due to the signal.

We generate signal B meson events using **Pythia v8** [25]; and **MadGraph v5** [26] with **FeynRules v2** [27] for the decays. (We have cross checked our event distributions using **EvtGen** [28].) Following Ref. [21], we compare the (mass dependent) efficiencies for selecting events in the channel $B_s^0 \rightarrow 3\mu^+3\mu^-$ with that for $B_s^0 \rightarrow 2\mu^+2\mu^-$. The former is shown in Tab. I, while we estimate the latter to be $\varepsilon_{2\mu^+2\mu^-} \sim 0.14$. The explanation for the smaller efficiencies for the six muon process is two fold. First, due to the larger number of final state tracks, there are more events with no single muon with $p_T > 1.7 \text{ GeV}$ which therefore do not pass the trigger; see Fig. 5. And second, there are more muons with at least one track with $p_T < 0.5 \text{ GeV}$ which is therefore not detected; see Fig. 6.

Given the absence of background, we can estimate the upper limit on the branching ratio of the new processes at $\sqrt{s} = 14 \text{ TeV}$ and luminosity \mathcal{L}' as

$$\mathcal{B}_{\max}^{3\mu^+3\mu^-} \sim \frac{\mathcal{B}_{\max}^{2\mu^+2\mu^-} \times \varepsilon_{2\mu^+2\mu^-}}{1.8 \times \varepsilon_{3\mu^+3\mu^-}} \times \frac{\mathcal{L}}{\mathcal{L}'} , \quad (22)$$

where $\mathcal{B}_{\max}^{2\mu^+2\mu^-}$ is the upper limit on $\mathcal{B}(B_s^0 \rightarrow 2\mu^+2\mu^-) = 2.5 \times 10^{-9}$, obtained in Ref. [19] with $\mathcal{L} = 3 \text{ fb}^{-1}$ and $\sqrt{s} = 8 \text{ TeV}$, under the same trigger and reconstruction criteria. The factor 1.8 stands for the approximated growth of the b production cross section from $\sqrt{s} = 8 \text{ TeV}$ to $\sqrt{s} = 14 \text{ TeV}$. The prospective bounds on the branching ratio of this new decay mode are given in Tab. I.

We also consider the channel $B^+ \rightarrow K^+3\mu^+3\mu^-$. In this case, on top of the selection criteria proposed before, we require the presence of a charged kaon which is also required to have $p_T > 0.5 \text{ GeV}$ and $2.5 < \eta < 5.0$. The corresponding efficiencies are shown in Tab. I. The limit on the branching ratio can be again obtained as

$$\mathcal{B}_{\max}^{3\mu^+3\mu^-K^+} \sim \frac{\mathcal{B}_{\max}^{2\mu^+2\mu^-} \times \varepsilon_{2\mu^+2\mu^-}}{1.8 \times 3.7 \times \varepsilon_{3\mu^+3\mu^-K^+}} \times \frac{\mathcal{L}}{\mathcal{L}'} , \quad (23)$$

where the factor 3.7 stands for the larger B^+ production cross section [29]. The bounds obtained this way are also shown in Tab. I. It is worth noting that the prospective limits on this channel are comparable or even more stringent than that on the decay mode without the extra meson (due mostly to the larger cross section, that compensates the smaller efficiency). This fact, together with the observation that theoretically this decay mode dominates for $m_2 \sim m_1$, strongly motivates searches for $B^+ \rightarrow K^+3\mu^+3\mu^-$.

For illustration, we translate the expected limits in Tab. I to the plane (g_{sb}, m_V) in Fig. 7 for definite values of g_{12} , m_1 , m_2 and m_{12} (when relevant). Prospects for the Upgrade II, defined by $\mathcal{L}' = 300 \text{ fb}^{-1}$, are also shown. It is interesting to see that with our proposed analyses we can easily test masses larger than 15 TeV , thereby outperforming constraints obtained from ΔM_s and completely probing the region in which the anomalies in lepton flavour universality can be explained.

Likewise, we also translate the aforementioned bounds to the plane (m_1, m_2) in Fig. 8, fixing $g_{sb} = 0.04$ as well as $m_V = 4 \text{ TeV}$. Such values are not yet excluded by measurements of ΔM_s ; see Refs. [30]. In both figures, only the weakest limits of Tab. I are used.

We also note that, if a signal is observed in these six-muon channels, the mass of the scalar particles involved could be reconstructed due to the outstanding detector resolution of the LHCb. To this aim, we provide two different algorithms, depending on whether $m_2 > 2m_1$ (in which case $a_2 \rightarrow a_1 a_1$) or rather $m_2 < 2m_1$ (and therefore $a_2 \rightarrow a_1 \mu^+ \mu^-$).

For the first case, we minimize the difference $|m_{11}^{\text{rec}} - m_{12}^{\text{rec}}| + |m_{12}^{\text{rec}} - m_{13}^{\text{rec}}|$, where m_i^{rec} is the invariant mass

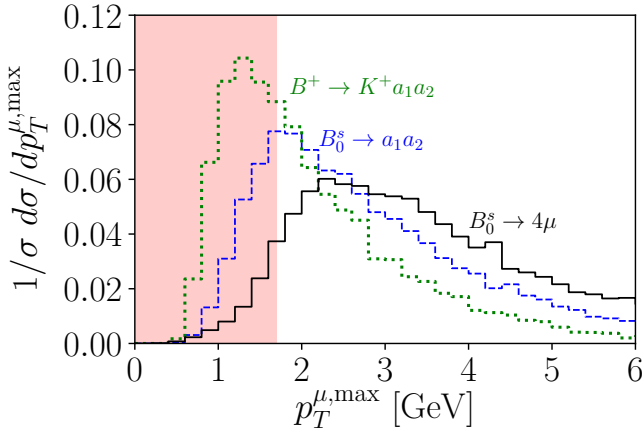


FIG. 5: Normalized distribution of the transverse momentum of the hardest muon for $B_s^0 \rightarrow a_1a_2$ and $B^+ \rightarrow K^+a_1a_2$ with $m_1 = 1$ GeV and $m_2 = 2.5$ GeV. These distributions are compared with the case $B_s^0 \rightarrow 2\mu^+2\mu^-$.

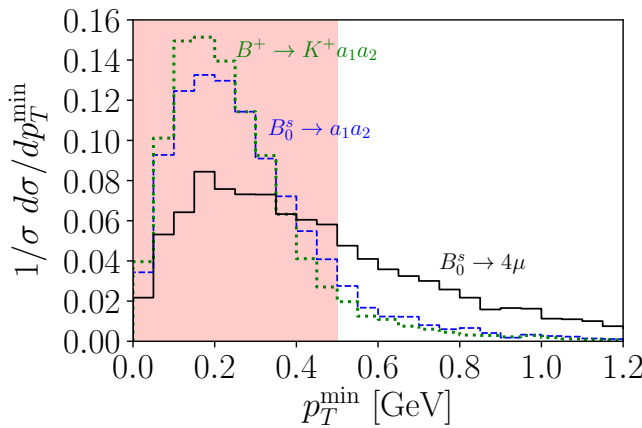


FIG. 6: Normalized distribution of the transverse momentum of the softest track for $B_s^0 \rightarrow a_1a_2$ and $B^+ \rightarrow K^+a_1a_2$ with $m_1 = 1$ GeV and $m_2 = 2.5$ GeV. These distributions are compared with the case $B_s^0 \rightarrow 2\mu^+2\mu^-$.

of each combination of opposite-sign muons. The two a_1 s that reconstruct the heavier scalar are those with the minimum ΔR among themselves; see Fig. 9 for an example.

Concerning the second case, the muon pairs reconstructing the two a_1 s are selected as those minimizing the difference $|m_{11}^{\text{rec}} - m_{12}^{\text{rec}}|$ among the three pairs of muons. Then, a_2 is reconstructed from the two muons not assigned to any a_1 and the a_1 that minimizes $\Delta R(p_1, p_{\mu\mu})$ (with p_1 its four-momentum and $p_{\mu\mu}$ the four-momentum of the aforementioned pair of muons); see Fig. 10.

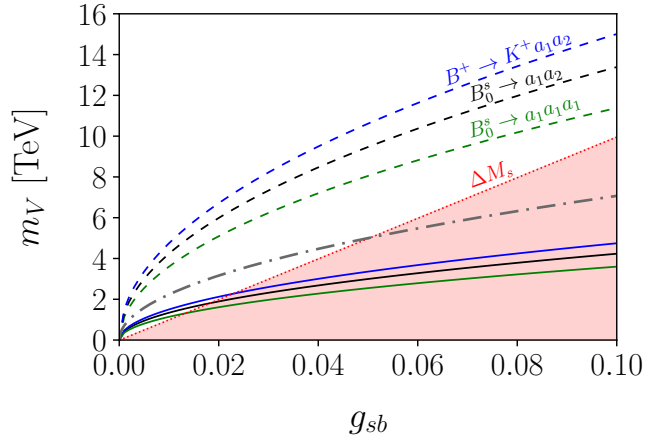


FIG. 7: Maximum value of m_V that can be tested in the searches for $B_s^0 \rightarrow 3\mu^+3\mu^-$ and $B^+ \rightarrow K^+3\mu^+3\mu^-$ at the current run of the LHCb (solid lines) and for Upgrade II (dashed lines). The red dotted line delimits the area excluded by measurements of ΔM_s . In the dash-dotted line the anomalies in R_K and R_{K^*} can be explained at the 1σ level assuming $g_{V\ell\ell} \sim 1$ [30]. We have fixed $g_{12} = 0.5$ as well as $m_1 = 1.2$ GeV. We have set $m_2 = 2.0$ GeV for both $B_s^0 \rightarrow a_1a_2$ and $B^+ \rightarrow K^+a_1a_2$. For $B_s^0 \rightarrow a_1a_1a_1$, we have fixed instead $m_2 = m_{12} = 5$ GeV.

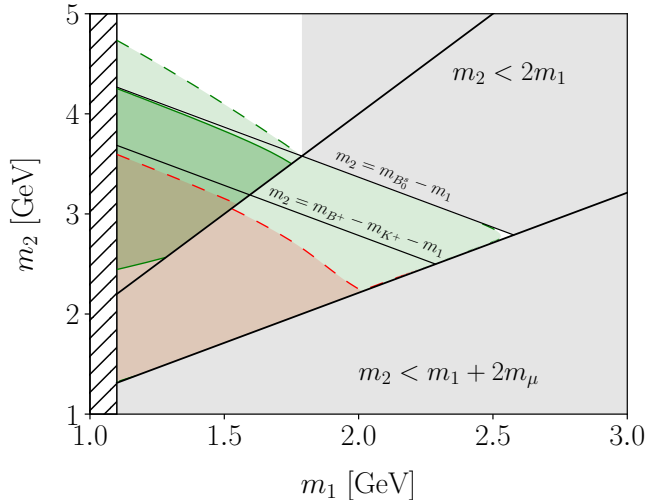


FIG. 8: Region of the plane (m_1, m_2) that can be tested at the current run of the LHCb (solid) and in Upgrade II (dashed) in searches for $B_s^0 \rightarrow 3\mu^+3\mu^-$ (green) and $B^+ \rightarrow K^+3\mu^+3\mu^-$ (red). We have fixed $g_{sb} = 0.04$, $m_V = 4$ TeV and $g_{12} = 0.5$, as well as $m_{12} = 1$ GeV (only relevant in the upper left region). The sensitivity is negligible in the slashed region.

IV. HIGH MASS REGIME AT THE LHC

In the high mass regime, $a_{1,2}$ can no longer be produced in the decay of B mesons. However, if V is light

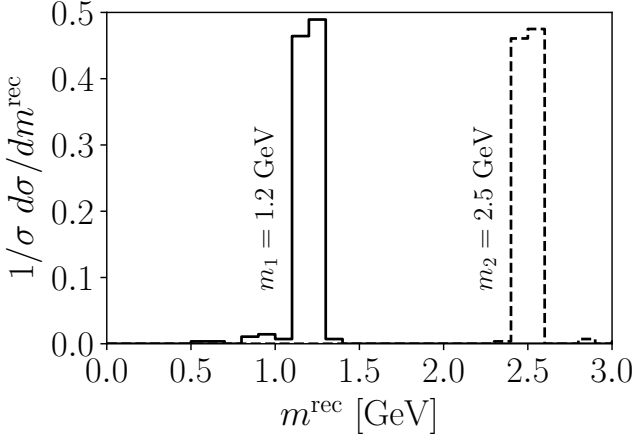


FIG. 9: Normalized distribution of the reconstructed m_1 (solid) and m_2 (dashed) for $m_2 > 2m_1$.

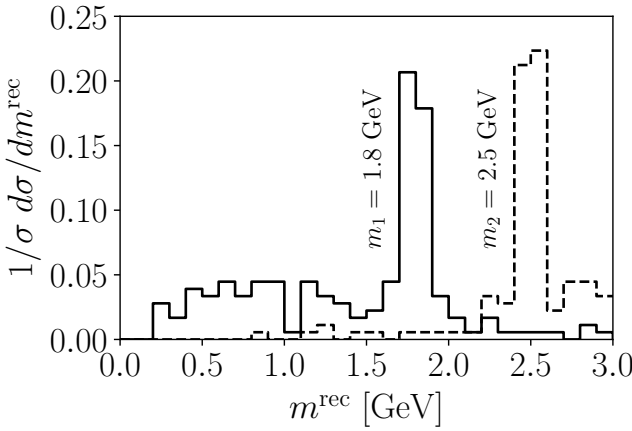


FIG. 10: Normalized distribution of the reconstructed m_1 (solid) and m_2 (dashed) for $m_2 < 2m_1$.

enough ($m_V \lesssim$ few TeV), it can be produced on shell at colliders, giving rise to $a_{1,2}$ pair production upon decay. The tree level signal cross section for $g_{qg} = 0.5$ and $g_{12} = 1$ ranges between ~ 0.04 pb and $\sim 10^{-5}$ pb for m_V between 1 and 5 TeV.

There are multilepton searches at the LHC which are very sensitive to this scenario. Most of them rely on substantial missing energy, being therefore not relevant for our model. In this work, we consider the signal region dubbed SR0A in the analysis of Ref. [31]. The main selection cuts of that study are (i) at least four isolated leptons; (ii) no hadronic taus; (iii) no pair of opposite-sign leptons with invariant mass in the range [81.2, 101.2] GeV; (iv) $m_{\text{eff}} > 600$ GeV, where m_{eff} stands for the scalar sum of the p_T of all leptons, jets with $p_T^j > 40$ GeV and missing energy.

Only hadronic tau candidates with $p_T^\tau > 20$ GeV are considered in (ii); jets are reconstructed using the anti-

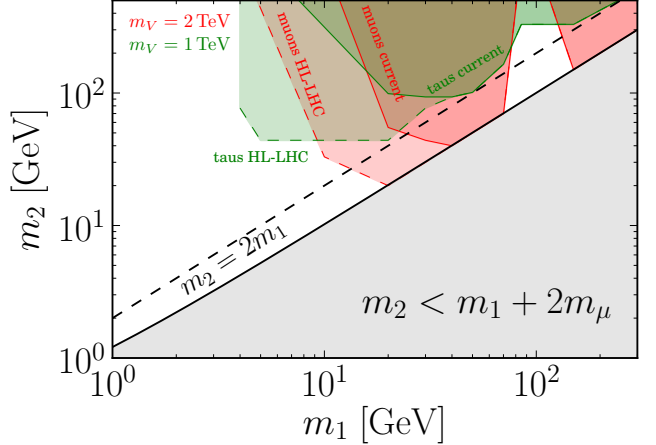


FIG. 11: Region in the plane (m_1, m_2) that is excluded by multilepton searches (solid red) and lepton-tau searches (solid green) [31]. The dashed lines represent the corresponding prospects at the HL-LHC. We have fixed $g_{qg} = 0.5$, $g_{12} = 1$.

k_t algorithm with $R = 0.4$. The experimental analysis reports the observation of 13 events, while 10.2 ± 2.1 are predicted in the background-only hypothesis. Using these numbers including the systematic uncertainty on the SM prediction, we obtain that the maximum number of allowed signal events is 12. Scaling the expected number of background events with the larger luminosity, and assuming the same uncertainty, the expected maximum number of signal events at the HL-LHC is 300.

We recast this analysis using homemade routines based on **ROOT** v5 [32], **HepMC** v2 [33] and **FasJet** v3 [34]. We define hadronic taus as jets with angular separation smaller than 0.2 from a true hadronic decayed tau lepton. We establish a flat tau-tagging efficiency of 0.5. We consider light leptons to be isolated if the hadronic activity around $\Delta R = 0.2$ of the corresponding lepton is smaller than 10% of its transverse momentum. On top of the cuts above, we require that the angular separation between any pair of muons is larger than 0.05, to simulate their correct reconstruction at detectors.

We generate signal events for $pp \rightarrow V \rightarrow a_1 a_2$ with the corresponding scalar decays with **MadGraph** v5 [26] with no parton level cuts. For the PDFs we use the NNPDF23L0 set [35]. Signal events are subsequently passed through **Pythia** v8 [25] to account for initial and final state radiation, fragmentation and hadronization effects.

If the light scalars couple mostly to the tau lepton (second scenario introduced in Section II), the aforementioned signal region has no sensitivity. We can rely instead on the signal region SR2 defined in the same experimental paper of Ref. [31], which requires (i) exactly two light leptons with invariant mass not in the range [81.2, 101.2] GeV; (ii) at least two hadronic taus with $p_T^\tau > 30$ GeV; $m_{\text{eff}} > 650$ GeV. The experimental collaboration reports the observation of 2 events; the SM prediction being 2.3 ± 0.8 . Using again the CL_s method,

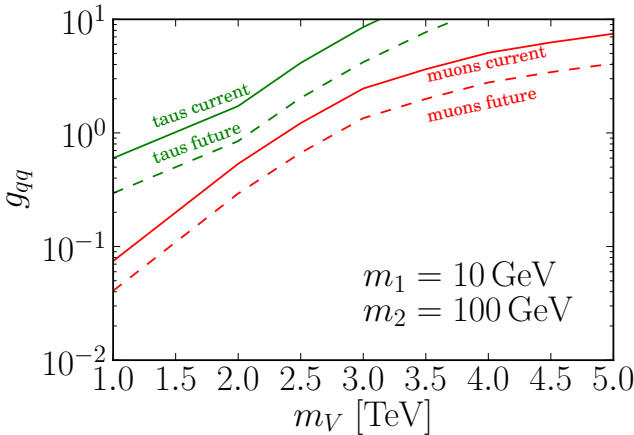


FIG. 12: Minimum value of g_{qq} that it is excluded by multilepton searches (solid red) and lepton-tau searches (solid green) [31]. The dashed lines represent the corresponding prospects at the HL-LHC. We have assumed $\mathcal{B}(V \rightarrow a_1 a_2) \sim 0.25$.

we obtain 6 (121) events as the current (future) maximum allowed signal.

We scan over 20 values of m_1 and m_2 in logarithmic scale in the range [1, 500] GeV, with special attention to low masses as well as masses close to the Z pole.

In Fig. 11 we depict the region in the (m_1, m_2) plane for $g_{qq} = 0.5$ and $g_{12} = 1$ that is already excluded in the muonphilic case and also in the case with couplings to taus. The exclusion prospects for the HL-LHC, defined by 3 ab^{-1} , are also shown. The tau analysis is much less constraining (mainly due to the small branching ratio to leptons), and thus we only show results for $m_V = 1 \text{ TeV}$.

The low sensitivity in the small m_1 region is due to muons being very collimated. (Decays into taus are furthermore forbidden for $m_1 \lesssim 4 \text{ GeV}$.) If it were possible to resolve muons with angular separations as small as 0.001, then almost the whole small mass range could be tested in the muonphilic case.

Likewise, the non excluded region around $m_1 \sim 100 \text{ GeV}$ results from the Z veto of the analysis. This region could be covered if the veto on the Z pole is removed and, instead of m_{eff} , the invariant mass of all final state observable objets (which in our signal, and contrary to the SUSY targets of the analysis, presents a narrow peak) is used. Such improvement would also extend the reach to smaller masses. It is therefore desirable that future updates of the experimental work consider different versions of the cut on m_{eff} .

In the same vein, in Fig. 12 we plot the minimum value of g_{qq} that can be tested for different values of m_V and for fixed values of $m_{1,2}$. We have also fixed g_{12} to the value for which $\mathcal{B}(V \rightarrow a_1 a_2) \sim 0.25$.

V. CONCLUSIONS

We have studied the phenomenology of light leptophilic scalars $a_{1,2}$ that couple to a heavy flavour violating (mostly $b - s$ like) spin-1 resonance V . We have shown that, under very mild conditions, a_2 decays mostly into a_1 , which subsequently decays into pairs of leptons. Thus, for scalar masses \lesssim few GeV, this scenario produces new B meson decays into six muons, namely $B_s^0 \rightarrow 3\mu^+ 3\mu^-$ and $B^+ \rightarrow K^+ 3\mu^+ 3\mu^-$. Interestingly, the later dominates over the second when $m_1 \sim m_2$. None of them has been explored experimentally; we have therefore proposed dedicated analyses to explore these signals at the LHCb. We have found that branching ratios as small as 6.0×10^{-9} (5.9×10^{-9}) for the first (second) process can be already tested with the current luminosity. Branching ratios hundred times smaller could be probed at the Upgrade-II of the LHCb.

For larger scalar masses, $a_{1/2}$ arise rather in the decay of V , which can be produced on shell at pp collisions at the LHC. Current multilepton searches in final states with muons (taus) constrain most of the parameter space for $m_1 \gtrsim 10 \text{ GeV}$ provided that $\sigma(pp \rightarrow V \rightarrow a_1 a_2) \gtrsim 0.001$ (0.01) pb. Smaller masses give rise to very collimated leptons (or jets) that are difficult to disentangle at detectors. However, at the HL-LHC, the reach can be extended to $m_1 \lesssim 5$. And even further if the current analyses cut on the invariant mass of all visible objets.

Finally, let us comment how these results would get modified if different flavour assumptions are made. To start with, if $a_{1,2}$ are not leptophilic but rather they couple to all SM fermions with Yukawa-like couplings, the branching ratio of a_1 into leptons would get reduced by one-to-two orders of magnitude. In turn, LHCb would be only sensitive to exotic branching ratios thousand times larger. (Note that such branching ratios are not excluded by any current measurement, though.) However, LHC searches in multilepton final states would lose almost all sensitivity in this case.

On the other hand, V might also induce $b - d$ transitions. In that case, we expect new rare decays such as $B^0 \rightarrow 3\mu^+ 3\mu^-$. The production cross section for B^0 is ~ 3.7 larger than for B_s^0 [29], from where we estimate that $\mathcal{B}(B^0 \rightarrow 3\mu^+ 3\mu^-) \gtrsim 1.6 \times 10^{-9}$ ($\sim 10^{-11}$) can be probed currently (in the Upgrade-II of the LHCb).

On the theory side, this channel vanishes also at tree level when $m_1 \sim m_2$. In this regime, we propose searching for $B_s^0 \rightarrow K^{*0} 3\mu^+ 3\mu^-$, with $K^{*0} \rightarrow K^+ \pi^-$; whose branching ratio is around 2/3 [36]. Upon performing an equivalent analysis to that described in Sec. III, we obtain efficiencies of about 2 times smaller, in comparison to the $B_s^0 \rightarrow 3\mu^+ 3\mu^-$ channel. Consequently, we estimate the LHCb reach to be $\mathcal{B}(B_s^0 \rightarrow K^{*0} 3\mu^+ 3\mu^-) \gtrsim 1.8 \times 10^{-8}$ currently, and again about hundred times stronger in the Upgrade-II.

At high scalar masses, the prospects are only slightly better than for $b - s$ transitions, because the production cross section for V at the LHC grows only by a very small

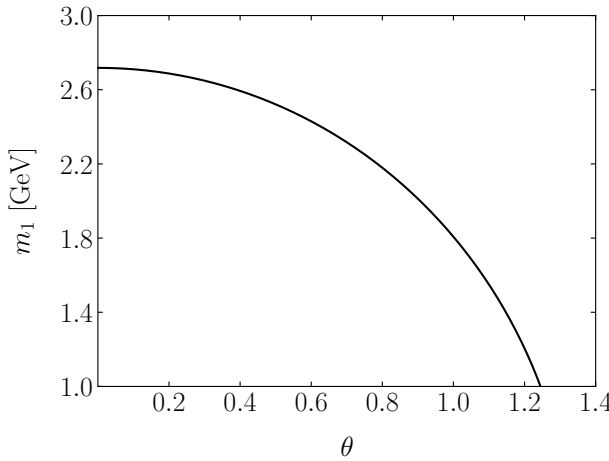


FIG. 13: *Mass of a_1 as a function of θ (for $f = 1$ TeV), obtained from the embedding of the left-handed leptons in the symmetric representation of $SO(7)$.*

factor. Both low and high energy searches are also more constraining than bounds on ΔM_d [37] on a wide region of the parameter space.

Overall, our study motivates new searches for $B_s^0 \rightarrow (K^{*+})3\mu^+3\mu^-$ and $B^+ \rightarrow K^+3\mu^+3\mu^-$ at the LHCb as well as small modifications of current multilepton and multitau analyses at CMS and ATLAS.

Acknowledgments

We are grateful to Ulrik Egede for previous collaboration that opened this new line of research. MC is sup-

ported by the Royal Society under the Newton International Fellowship programme. MR is supported by Fundação para a Ciência e Tecnologia (FCT) under the grant PD/BD/142773/2018 and also acknowledges financing from LIP (FCT, COMPETE2020-Portugal2020, FEDER, POCI-01-0145-FEDER-007334). MR would like to thank the IPPP Durham for hospitality where the main part of this work was carried out. MS acknowledges the hospitality of the University of Tuebingen and support of the Humboldt Society during the completion of parts of this work.

Appendix A: Concrete composite Higgs model

Non-minimal CHMs is the context where heavy vector bosons and new light scalars, separated by a large mass gap, arise more naturally. The reason is that the latter are pseudo Nambu Golstone bosons (pNGBs) from the spontaneous breaking of \mathcal{G}/\mathcal{H} , at a scale $f \sim$ TeV.

The smallest coset for which the scalar sector consists of the Higgs degrees of freedom as well as two SM singlets is $SO(7)/SO(6)$ [7–9]. The corresponding 15 unbroken and 6 broken generators, T and X respectively, can be written as:

$$\begin{aligned} T_{ij}^{mn} &= -\frac{i}{\sqrt{2}} (\delta_i^m \delta_j^n - \delta_i^n \delta_j^m) , \quad m < n \in [1, 6] ; \\ X_{ij}^{mn} &= -\frac{i}{\sqrt{2}} (\delta_i^m \delta_j^7 - \delta_i^7 \delta_j^m) , \quad m \in [1, 6] . \end{aligned} \quad (\text{A1})$$

Without loss of generality, the pNGB matrix can be written as

$$U = \begin{bmatrix} \mathbf{1}_{3 \times 3} & & & & \\ & 1 - h^2/(f^2 + f^2 \Sigma) & -ha_1/(f^2 + f^2 \Sigma) & -ha_2/(f^2 + f^2 \Sigma) & h/f \\ & -ha_1/(f^2 + f^2 \Sigma) & 1 - a_1^2/(f^2 + f^2 \Sigma) & -a_1 a_2/(f^2 + f^2 \Sigma) & a_1/f \\ & -ha_2/(f^2 + f^2 \Sigma) & -a_1 a_2/(f^2 + f^2 \Sigma) & 1 - a_2^2/(f^2 + f^2 \Sigma) & a_2/f \\ & -h/f & -a_1/f & -a_2/f & \Sigma \end{bmatrix} , \quad (\text{A2})$$

with $\Sigma^2 = 1 - (h^2 + a_1^2 + a_2^2)/f^2$.

Following the partial compositeness paradigm [38], the couplings of $a_{1,2}$ to the SM fermions, as well as the scalar potential, depend on the quantum numbers of the composite operators that the SM fermions mix with breaking the global symmetry. Or equivalently, they depend on how the SM fermions are embedded in representations of $SO(7)$.

We assume that $q_L + u_R \sim \mathbf{7} + \mathbf{21}$. Likewise, we assume

that $l_L + e_R \sim \mathbf{27} + \mathbf{1}$. Explicitly, $L_L \equiv \nu_L \Lambda^e + e_L \Lambda^\nu$:

$$L_L = \frac{1}{2} \begin{pmatrix} 0_{4 \times 4} & \theta \mathbf{v}_1^T & \gamma \mathbf{v}_2^T & \mathbf{v}_2^T \\ \theta \mathbf{v}_1 & 0 & 0 & 0 \\ \gamma \mathbf{v}_2 & 0 & 0 & 0 \\ \mathbf{v}_2^T & 0 & 0 & 0 \end{pmatrix} , \quad (\text{A3})$$

where the vectors read $\mathbf{v}_1 = (e_L, -ie_L, \nu_L, i\nu_L)$ and $\mathbf{v}_2 = (ie_L, e_L, i\nu_L, -\nu_L)$ and θ and γ are real parame-

ters. (Note that the different embeddings for quarks and leptons is primarily justified by the fact that the lepton and quark masses and mixings are completely different.)

The scalar potential can be written as $V(h, a_{1,2}) = V_q(h, a_{1,2}) + V_l(h, a_{1,2})$, where the first and second contributions of the RHS come from loops of quarks and leptons, respectively. It can be also shown that the quark sector respects a symmetry $a_{1,2} \rightarrow -a_{1/2}$, as well as the shift symmetry of the singlets. Consequently, $V_q(h, a_{1,2}) = V_q(h)$. It is completely fixed by the measurements of the Higgs mass and its VEV.

The only model dependence come from $V_l(h, a_{1,2})$, which to leading order in the expansion in the global symmetry breaking parameters reads:

$$V_l \sim c_1 f^4 \left[(\Lambda_D^{\mathbf{1}*})^\alpha (\Lambda_D^{\mathbf{1}})_\alpha \right] + c_2 f^4 \left[(\Lambda_D^{\mathbf{6}*})_i^\alpha (\Lambda_D^{\mathbf{6}})_\alpha^i \right],$$

where the dressed spurion reads $\Lambda_D^\alpha \equiv U^T \Lambda^\alpha U$ with $\alpha = e, \nu$. (The indices **1** and **6** indicate the projection into the singlet and the sextuplet in the decomposition **27** = **1** + **6** + **20** from $SO(7)$ to $SO(6)$.) The constants c_1 and c_2 are free parameters encoding the (unknown) details on the strongly coupled UV. Writing explicitly the one-loop induced potential, we find:

$$\begin{aligned} V_l = & 4f^3 c_2 \gamma \Sigma a_2 + 2f (c_1 - 2c_2) \gamma \Sigma a_2 h^2 \\ & + \frac{1}{2} c_2 f^2 \left[\left(\gamma^2 + \theta^2 - 7 + 2 \frac{c_1}{c_2} \right) h^2 \right. \\ & \left. + 4(\theta^2 - 1) a_1^2 + 4(\gamma^2 - 1) a_2^2 \right] \\ & + (c_1 - 2c_2) \left[(\theta^2 - 1) a_1^2 + (\gamma^2 - 1) a_2^2 - h^2 \right] h^2. \end{aligned} \quad (\text{A4})$$

We further expand this expression in powers of $1/f$, and keep only terms up to dimension four:

$$\begin{aligned} V_l \sim & 4f^3 c_2 \gamma a_2 + 2f^2 c_2 \left[(\gamma^2 - 1) a_2^2 + (\theta^2 - 1) a_1^2 \right] \\ & + 2f \gamma \left[(c_1 - 3c_2) a_2 h^2 - c_2 (a_1^2 + a_2^2) a_2 \right] \\ & + (c_1 - 2c_2) \left[(\theta^2 - 1) a_1^2 + (\gamma^2 - 1) a_2^2 \right] h^2 + \dots \end{aligned} \quad (\text{A5})$$

where the three dots encode terms involving the Higgs boson solely.

The requirements $c_1 \sim 3c_2$ and $\gamma \sim 1$ make the interactions between a_2 and the Higgs (in particular mixings) very small. In order to avoid bounds from Higgs searches, we restrict to this case hereafter. The tadpole can then be removed by the field redefinition $a_2 \rightarrow a_2 + \sqrt{2/3}f$.

Let us also fix $f = 1$ TeV, as well as $c_2 \sim g_*^2 y_l^2 / (4\pi)^2 \sim 10^{-6}$. The latter is the value expected from SILH power counting [39] for $g_* \sim 3$, with g_* the typical strong coupling between composite resonances. This choice fixes both m_2 and m_{12} to ~ 3.1 GeV and ~ 0.002 GeV, respectively; while m_1 depends solely on θ . We compute numerically this dependence and it is depicted in Fig. 13.

On another front, the Yukawa Lagrangian to dimension five reads:

$$\begin{aligned} L_Y = & y f \bar{l}_L^\alpha (\Lambda_D^\alpha)_{77}^\dagger e_R + \text{h.c.} \\ = & y \bar{e} \bar{l}_L H e_R \left[1 + \frac{1}{f} (a_2 - i\theta a_1) + \dots \right]. \end{aligned} \quad (\text{A6})$$

The vector resonance associated to the generator T^{56} is the only one that couples to $a_{1,2}$. We identify it with V . The interaction between V and the pNGBs is entirely determined by the CCWZ formalism [40–42], reading:

$$L = \frac{1}{2g_*^2} m_V^2 (g_* V_\mu^a - e_\mu^a)^2, \quad (\text{A7})$$

where e_μ is the trace of the Maurer-Cartan form ω along the unbroken generators:

$$\omega_\mu = -i U^\dagger \partial_\mu U = d_\mu^a X_a + e_\mu^a T_a. \quad (\text{A8})$$

We expect $m_V \sim g_* f$. Therefore, the interaction between the vector resonance and the light scalars reads:

$$L_{int} = \sqrt{2} g_* \frac{V_\mu a_2 \overleftrightarrow{\partial}^\mu a_1}{1 + \Sigma} \sim \frac{g_*}{\sqrt{2}} V_\mu a_2 \overleftrightarrow{\partial}^\mu a_1. \quad (\text{A9})$$

Finally, the vector resonance can not couple directly to the left-handed quarks. The coupling g_{qq} is therefore suppressed by $v^2/f^2 \lesssim 0.1$.

Altogether, this model matches into the parameterization in Eq. 1. For example, let us take $\theta = 1.2$. We obtain: $m_1 \sim 1.3$ GeV, $m_2 \sim 3.1$ GeV, $m_{12} \sim 0.002$ GeV, $g_{qq} \sim 0.1$, $g_{12} \sim 2$, $g_2 \sim 0.17$, $g_1 \sim 0.22$.

These numbers are also obtained if the leptons are embedded in **7** + **7**.

[1] M. Chala, *A critical assessment of the status of LHC searches for new physics*, PoS **CORFU2017** (2018) 047.

[2] D. B. Kaplan and H. Georgi, *$SU(2) \times U(1)$ Breaking by Vacuum Misalignment*, Phys. Lett. **136B** (1984) 183–186.

[3] D. B. Kaplan, H. Georgi and S. Dimopoulos, *Composite Higgs Scalars*, Phys. Lett. **136B** (1984) 187–190.

[4] B. Gripaios, A. Pomarol, F. Riva and J. Serra, *Beyond the Minimal Composite Higgs Model*, JHEP **04** (2009) 070, [0902.1483].

[5] L. Vecchi, *The Natural Composite Higgs*, 1304.4579.

[6] V. Sanz and J. Setford, *Composite Higgses with seesaw EWSB*, *JHEP* **12** (2015) 154, [[1508.06133](#)].

[7] M. Chala, G. Nardini and I. Sobolev, *Unified explanation for dark matter and electroweak baryogenesis with direct detection and gravitational wave signatures*, *Phys. Rev.* **D94** (2016) 055006, [[1605.08663](#)].

[8] R. Balkin, M. Ruhdorfer, E. Salvioni and A. Weiler, *Charged Composite Scalar Dark Matter*, *JHEP* **11** (2017) 094, [[1707.07685](#)].

[9] L. Da Rold and A. N. Rossia, *The Minimal Simple Composite Higgs Model*, [1904.02560](#).

[10] C. Niehoff, P. Stangl and D. M. Straub, *Violation of lepton flavour universality in composite Higgs models*, *Phys. Lett.* **B747** (2015) 182–186, [[1503.03865](#)].

[11] C. Niehoff, P. Stangl and D. M. Straub, *Direct and indirect signals of natural composite Higgs models*, *JHEP* **01** (2016) 119, [[1508.00569](#)].

[12] A. Carmona and F. Goertz, *Lepton Flavor and Nonuniversality from Minimal Composite Higgs Setups*, *Phys. Rev. Lett.* **116** (2016) 251801, [[1510.07658](#)].

[13] E. Megias, G. Panico, O. Pujolas and M. Quiros, *A Natural origin for the LHCb anomalies*, *JHEP* **09** (2016) 118, [[1608.02362](#)].

[14] I. Garcia Garcia, *LHCb anomalies from a natural perspective*, *JHEP* **03** (2017) 040, [[1611.03507](#)].

[15] F. Sannino, P. Stangl, D. M. Straub and A. E. Thomsen, *Flavor Physics and Flavor Anomalies in Minimal Fundamental Partial Compositeness*, *Phys. Rev.* **D97** (2018) 115046, [[1712.07646](#)].

[16] A. Carmona and F. Goertz, *Recent B physics anomalies: a first hint for compositeness?*, *Eur. Phys. J.* **C78** (2018) 979, [[1712.02536](#)].

[17] M. Chala and M. Spannowsky, *Behavior of composite resonances breaking lepton flavor universality*, *Phys. Rev.* **D98** (2018) 035010, [[1803.02364](#)].

[18] S. V. Demidov and D. S. Gorbunov, *Flavor violating processes with sgoldstino pair production*, *Phys. Rev.* **D85** (2012) 077701, [[1112.5230](#)].

[19] LHCb collaboration, R. Aaij et al., *Search for decays of neutral beauty mesons into four muons*, *JHEP* **03** (2017) 001, [[1611.07704](#)].

[20] A. E. Nelson and J. Scholtz, *Heavy flavor and dark sector*, *Phys. Rev.* **D91** (2015) 014009, [[1311.0040](#)].

[21] M. Chala, U. Egede and M. Spannowsky, *Searching new physics in rare B-meson decays into multiple muons*, *Eur. Phys. J.* **C79** (2019) 431, [[1902.10156](#)].

[22] J. Liu, C. E. M. Wagner and X.-P. Wang, *A light complex scalar for the electron and muon anomalous magnetic moments*, *JHEP* **03** (2019) 008, [[1810.11028](#)].

[23] K. Cheung, C.-W. Chiang, N. G. Deshpande and J. Jiang, *Constraints on flavor-changing Z' models by B(s) mixing, Z' production, and B(s) —> mu+ mu-*, *Phys. Lett.* **B652** (2007) 285–291, [[hep-ph/0604223](#)].

[24] P. Ball and R. Zwicky, *New results on B → π, K, η decay formfactors from light-cone sum rules*, *Phys. Rev.* **D71** (2005) 014015, [[hep-ph/0406232](#)].

[25] T. Sjstrand, S. Ask, J. R. Christiansen, R. Corke, N. Desai, P. Ilten et al., *An Introduction to PYTHIA 8.2*, *Comput. Phys. Commun.* **191** (2015) 159–177, [[1410.3012](#)].

[26] J. Alwall, R. Frederix, S. Frixione, V. Hirschi, F. Maltoni, O. Mattelaer et al., *The automated computation of tree-level and next-to-leading order differential cross sections, and their matching to parton shower simulations*, *JHEP* **07** (2014) 079, [[1405.0301](#)].

[27] C. Degrande, C. Duhr, B. Fuks, D. Grellscheid, O. Mattelaer and T. Reiter, *UFO - The Universal FeynRules Output*, *Comput. Phys. Commun.* **183** (2012) 1201–1214, [[1108.2040](#)].

[28] D. J. Lange, *The EvtGen particle decay simulation package*, *Nucl. Instrum. Meth.* **A462** (2001) 152–155.

[29] LHCb collaboration, R. Aaij et al., *Measurement of b-hadron production fractions in 7 TeV pp collisions*, *Phys. Rev.* **D85** (2012) 032008, [[1111.2357](#)].

[30] L. Di Luzio, M. Kirk and A. Lenz, *Updated B_s-mixing constraints on new physics models for b → sl⁺l⁻ anomalies*, *Phys. Rev.* **D97** (2018) 095035, [[1712.06572](#)].

[31] ATLAS collaboration, M. Aaboud et al., *Search for supersymmetry in events with four or more leptons in √s = 13 TeV pp collisions with ATLAS*, *Phys. Rev.* **D98** (2018) 032009, [[1804.03602](#)].

[32] R. Brun and F. Rademakers, *ROOT: An object oriented data analysis framework*, *Nucl. Instrum. Meth.* **A389** (1997) 81–86.

[33] M. Dobbs and J. B. Hansen, *The HepMC C++ Monte Carlo event record for High Energy Physics*, *Comput. Phys. Commun.* **134** (2001) 41–46.

[34] M. Cacciari, G. P. Salam and G. Soyez, *FastJet User Manual*, *Eur. Phys. J.* **C72** (2012) 1896, [[1111.6097](#)].

[35] R. D. Ball et al., *Parton distributions with LHC data*, *Nucl. Phys.* **B867** (2013) 244–289, [[1207.1303](#)].

[36] PARTICLE DATA GROUP collaboration, M. Tanabashi et al., *Review of Particle Physics*, *Phys. Rev.* **D98** (2018) 030001.

[37] P. Foldenauer and J. Jaeckel, *Purely flavor-changing Z' bosons and where they might hide*, *JHEP* **05** (2017) 010, [[1612.07789](#)].

[38] D. B. Kaplan, *Flavor at SSC energies: A New mechanism for dynamically generated fermion masses*, *Nucl. Phys.* **B365** (1991) 259–278.

[39] G. F. Giudice, C. Grajean, A. Pomarol and R. Rattazzi, *The Strongly-Interacting Light Higgs*, *JHEP* **06** (2007) 045, [[hep-ph/0703164](#)].

[40] S. R. Coleman, J. Wess and B. Zumino, *Structure of phenomenological Lagrangians. 1.*, *Phys. Rev.* **177** (1969) 2239–2247.

[41] C. G. Callan, Jr., S. R. Coleman, J. Wess and B. Zumino, *Structure of phenomenological Lagrangians. 2.*, *Phys. Rev.* **177** (1969) 2247–2250.

[42] G. Panico and A. Wulzer, *The Composite Nambu-Goldstone Higgs*, *Lect. Notes Phys.* **913** (2016) pp.1–316, [[1506.01961](#)].